한국

The Effect of Sliding Velocity on the

Mechanical Response of an Artificial Joint in

Topopah Spring Member Tuff

William A. Olsson
Geomechanics Department
Sandia National Laboratories

ABSTRACT

A smooth artificial joint in Topopah Spring Member tuff was sheared at constant normal stress at velocities from 0 to 100 μm/s to determine the velocity-dependence of shear strength. Two different initial conditions were used: (1) unprimed—the joint had been shear stress-free since last application of normal stress, and before renewed shear loading; and (2) primed—the joint had undergone a slip history after application of normal stress, but before the current shear loading. Observed steady-state rate effects were found to be about 3 times larger than for some other silicate rocks. These different initial conditions affected the character of the stress-slip curve immediately after the onset of slip. Priming the joint causes a peak in the stress-slip response followed by a transient decay to the steady-state stress, i.e., slip weakening. Slide-hold-slide tests exhibit time-dependent strengthening. When the joint was subjected to constant shear stress, no slip was observed; that is, joint creep did not occur. One set of rate data was collected from a surface submerged in tap water; the friction was higher for this surface, but the rate sensitivity was the same as that for surfaces tested in the air-dry condition.

This report was prepared under the Yucca Mountain Project WBS number 1.2.3.2.7.1.4. The data in this report was developed subject to QA controls in QAGR S1232714; the data is not qualified and is not to be used for licensing.

Contents

List of Figures

1 Introduction

The Topopah Spring Member of the Paintbrush Tuff within Yucca Mountain, Nevada, has been selected as a potential repository of high-level nuclear wastes. The Yucca Mountain Site Characterization Project (YMP) of the Office of Civilian Radioactive Waste Managememnt (OCRWM) Program has been assigned the task of determining the suitability of the Yucca Mountain site. Among the concerns being investigated, the characterization of the mechanical properties of the host rock has direct relevance to repository design, and to pre- and post-closure performance assessment.

Licensing of a nuclear-waste repository by the Nuclear Regulatory Commission (NRC) requires, among other things, demonstration of the long-term usability of the underground portion of the repository. Such a demonstration involves analysis of the mechanical response of the rock mass to the presence of underground openings and heat-producing waste over long periods of time. This report presents data on the time-dependent properties of a fracture as measured in rate-stepping and creep experiments in support of design and preformance stability issues. The test material was taken from a block of welded, devitrified Topopah Spring tuff (Price *et al.*, 1987).

Mechanical discontinuities such as faults, bedding planes, or joints are important mechanical constituents of most rock masses; they increase the compliance and decrease the strength of the rock mass. Stress changes and slip-induced dilation can affect the contributions of mechanical discontinuities to fluid permeability of the rock mass (Olsson, 1992; Olsson and Brown, 1993). Furthermore, the constitutive response of joints in silicate rocks is of a type that can lead to dynamic instabilities under a range of conditions. These instabilities are referred to as "stick-slip" and manifest themselves in experiments as jerky sliding accompanied by stress drops. This behavior on a larger scale is thought to be analogous to earthquakes (Brace and Byerlee, 1966). It has been shown (Wong, 1992) that most mine seismicity, e.g., rock bursts and bumps, is due to slip on geologic discontinuities. Further, it has been established that slip on joints in Grouse Canyon welded tuff is accompanied by acoustic emissions (Holcomb and Teufel, 1982) and therefore it is important to explain this aspect of time-dependent joint behavior of tuff.

For simplicity, the term "joint" is used throughout this report, but the results apply to any interface in rock with vanishingly small tensile strength.

The shear resistance of a joint depends on the normal stress history across it, the sliding velocity history, the temperature, the roughness, and the presence of water and gouge. It is generally accepted that normal stress is the dominant factor controlling the shear strength of a given joint and that all other effects have second order influence. This report focuses on time- or rate-dependence. It is important to understand that these effects, though lesser in magnitude of associated stress changes, can have important consequences. For example, it has been established that the details of the rate-dependence part of the constitutive description can either enhance or suppress instabilities in slip (Gu, *et al.*, 1984; Rice and Ruina, 1983; Ruina, 1983). As such, these rate effects have a direct
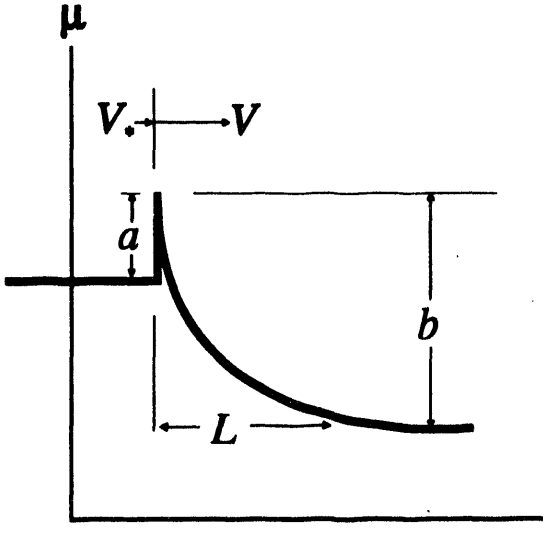
Figure 1: Definition sketch for constitutive parameters a, b, and L. The imposed load-point velocity is such that $V_* < V$.

bearing on mine seismicity.

Constitutive equation development for the time-dependent slip of interfaces at invariable normal stress is limited at this time to encompassing the effects of velocity, the history of velocity and the state of the surface. The theory is purely phenomenological in that no underlying physical process has been identified that predicts the response.

1.1 Review of the Constitutive Equations

The resistance to slip τ is coupled to the normal stress σ to dominant order through the coefficient of friction μ according to the slip condition

$$\tau - \mu\sigma \leq 0. \tag{1}$$

When the net shear stress $\tau - \mu\sigma$ is less than zero there is no slip. When absolute equality holds, the rate effects enter the problem. Whether creep will occur for $\tau - \mu\sigma < 0$ is not yet well-documented. This report presents results of several short-term creep tests, and this issue is now being investigated in long-term (about 3 months) creep tests. When the net shear stress on a joint is less than zero, the rock mass response in shear is approximately the same as that of the intact rock.

There are two classes of frictional constitutive laws: slip-dependence (often referred to as slip-weakening) and rate- and state-dependence. Slip-dependence laws embody monotonic surface

evolution that may be related to damage accumulation. These laws have the defect that there is no explicit rate-dependence and observed repeated instabilities are not predicted. The rate- and state-dependence law can predict repeated behavior, but may not be appropriate for the initial stages of slip when strong surface evolution to a steady-state takes place. Fracture behavior spans both types of description. In general terms, frictional slip has elements of both discrete memory (slip-dependence) and fading memory (rate- and state-dependence) of past stress and velocity (Olsson, 1987b).

The rate effects described herein are best discussed within the context of the rate- and state-dependence model. Experimental work of Dieterich (1972, 1978, 1979) followed by Ruina (1980, 1983) and Dieterich (1981) led to the development of the currently accepted formulation for effects of sliding velocity history and time on joint behavior (Ruina, 1983; Rice and Ruina, 1983). Rice and his coworkers (Gu et al., 1984; Rice and Gu, 1983) implemented the constitutive equations into predictive stability analyses. Tullis and Weeks (1986) gave an account of results from rotary shear experiments on granite within the framework of this theory.

The constitutive model is based on observed changes in friction during and immediately following abrupt changes in velocity. The state of the surface is included through time-evolving state variables. The basic equations describing this rate- and state-dependent behavior at constant normal stress and when the slip condition is satisfied (1) are:

$$\mu = \mu_* + b_i\Psi_i + a\ln(V/V_*),\tag{2}$$

$$d\Psi_i/dt = -(V/L_i)[\Psi_i + \ln(V/V_*)].\tag{3}$$

In these equations, V is the sliding velocity, Ψ_i are state variables that evolve with time, μ_* is the friction at an arbitrary reference velocity V_*. The parameters a and b_i are constants to be determined, and the L_i are the distances over which the Ψ_i evolve. A simple experiment, such as shown in Figure 1, provides all the parameters.

Differentiation of the constitutive equations, simplified to one state variable ($i = 1$), leads to the following definitions of the variables a, b, and L (Fig. 1):

$$\left.\frac{\partial\mu}{\partial\ln V}\right|_{\Psi} = a\tag{4}$$

$$\frac{d\mu^{ss}}{d\ln V} = a - b\tag{5}$$

$$\left.\frac{\partial\mu}{\partial x}\right|_V = -\frac{\mu - \mu^{ss}}{L}.\tag{6}$$

Thus, a is the instantaneous response following a jump in the velocity, and $a - b$ measures the difference between the current and former steady-state values of friction. The steady-state friction,
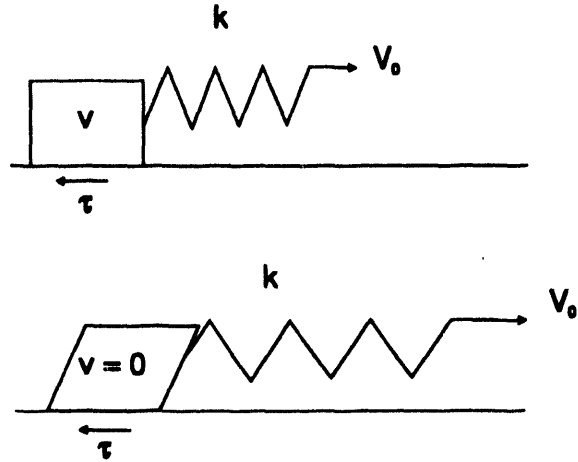
Figure 2: Spring and block analogue to sliding of laboratory-sized joint. V_0 is the load-point velocity imposed by the loadframe, τ is the resisting shear traction, and V is the velocity of the block.

$\Psi = 0$, is

$$\mu^{ss} = \mu_* + (a - b)\ln(V/V_*). \tag{7}$$

If $\mu^{ss} < \mu_*$, then the response is said to be velocity weakening and $a - b < 0$. If $\mu^{ss} > \mu_*$, then the response is said to be velocity strengthening and $a - b > 0$. The type of response observed for silicate rocks depends on the normal stress—low normal stress promotes stick-slip behavior, and high normal stress promotes velocity strengthening. Blanpied et al. (1987) have found that for V_0 greater than about 100 μm/s, $a - b$ becomes positive, implying stability. Elevated temperatures also can promote stable response (Blanpied et al., 1991). It is not clear whether the state changes, $d\Psi \neq 0$, when the surfaces are in stationary contact to begin with, that is, when the previous steady state is actually the zero velocity history ($V = 0$, for all previous time). The evolution of Ψ is clear when the first and second steady-states are at finite velocities, but if $V_* = 0$ for a long time, does the state change?

Joints are interfaces embedded in a deformable medium and as such do not necessarily slide over their whole extent simultaneously. Therefore, inhomogeneous slip may be important in the field and in the laboratory (Olsson, 1984). Rice (1983) has shown that the inhomogeneous slip regime associated with the advancing slip zone boundary is of the order of 1 metre. For the rotary shear configuration in particular, it has been shown that slippage is essentially uniform (Olsson, 1987b). Evidently, for normal laboratory sample dimensions, it is permissible to interpret laboratory friction data in terms of a rigid block being slid over a smooth surface by a force pulling on a spring connected to the block (Fig. 2).

The force, displacement, and velocity V_0 at the distal end of the spring are called the load-point values. In the load frame used in this investigation, the torque and angular displacement are applied at one end of the loading column while the joint is at the other. Thus, constant displacement rates

4

are applied through the elastic loading column, and because of the finite stiffness of the column there may be a difference in the velocity of sliding and the applied velocity, $V_0 - V$. This compliant load application is similar to a joint being loaded by the surrounding compliant rock and, in this sense, the laboratory experiment simulates nature. The difference in load-point velocity compared to joint-wall relative velocity emphasizes the importance of separating constitutive response of the joint from the loading-system response.

The spring-block system is described by

$$\frac{d\tau}{dt} = k(V_0 - V) \tag{8}$$

where k is the spring constant, V_0 is the velocity at the load point, and V is the velocity of the block. If the system unloading stiffness k is such that

$$k \leq \frac{b-a}{L}, \tag{9}$$

then the system will be prone to instablility in the form of jerky slipping and sudden stress drops (Dieterich, 1978). This shows how the value of the constitutive parameters b and a when combined with the properties of the loading system are important to stability. Natural joints will have different properties depending on geometric factors, mainly the roughness and degree of interlocking of adjacent joint walls. A different problem not considered here is the effect of gouge on the behavior of joints. Because the response of a joint depends on some convolution of the basic smooth-surface friction with its topographic properties, it is most illuminating to measure the magnitude of the effects of the variables on the smooth rock surfaces first, and then introduce the very complicated problem of surface roughness. The focus here is on the effects of sliding velocity, the history of the velocity, and the initial state of the sliding surface on strength of smooth surfaces.

2   Experimental Technique and Sample Preparation

The results reported here were obtained in rotary shear experiments (Christensen *et al.*, 1974; Kutter, 1974; Olsson, 1987ab, 1988ab, 1990, 1992; Xu and Frietas, 1988; Tullis and Weeks, 1986; Weeks and Tullis, 1985; Yoshioka and Scholz, 1989). In this type of experiment, the sample is composed of two, short, hollow tubes of rock that are pressed together under controlled load, and then torque is applied to cause sliding on the interface (Fig. 3). Further details may be obtained from (Olsson, 1987a).

The sample used in this study was sawed, then ground flat and perpendicular to the cylinder axis. Outside and inside diameters were 88.9 mm and 50.8 mm, respectively. The short (approx. 50 mm) cylinders were cemented to metal disks with epoxy, and then reground to ensure that the joint was parallel to the surfaces of the metal disks. The joint surfaces were then sandblasted to
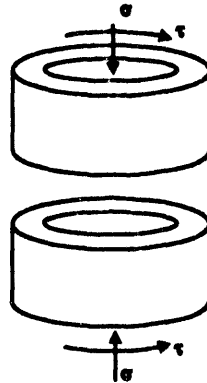
Figure 3: Sample configuration for rotary shear experiments on joints.

a dull finish. Before the experiments, the joint was slid back and forth under low normal stress of around 1 MPa to "run-in" the surface. This procedure stabilizes the stress-slip response loops and makes them reproducible under nominally identical test conditions. The experiments were performed on clean surfaces that had been run-in. In this report, the terms "mean slip" and "slip" are used interchangeably for angle of rotation in radians times $(D_o + D_i)/4$, where D_o and D_i are the outer and inner diameters, respectively. The load-point slip was corrected to slip by subtracting τ/(unloading slope) from the measured displacements. This difference in the stress-slip reponse when using these two measures can be seen by comparing the initial loading portion of the curves in Figures 4 and 5.

3 Results and Discussion

3.1 The effect of Velocity Changes at Constant Normal Stress

It had been found in earlier studies on tuff (Olsson, 1987a, 1988b) that there exist two recognizable initial conditions for smooth, topographically uncorrelated surfaces under the same test conditions: *unprimed* and *primed*. To create the unprimed initial condition, the initially separated joint walls are brought together and normal stress is applied; then the shear test is performed. In the primed condition, the joint has undergone some slip at non-zero normal stress, but now the contact is stationary; the shear test is performed on this joint. The response for these two states to increasing shear stress (Fig. 4) is significantly different. For the unprimed joint, the shear stress rises steadily to the initial slip stress (analogous to the initial yield stress in solids), then rolls over to the steady-sliding value, which remains essentially constant thenceforth. On the other hand, for the primed surface, the shear stress rises steadily to the initial slip stress, then breaks over discontinuously to the steady sliding value. Often, a peak in stress is observed, followed by a rapid decline to the steady sliding value. The difference in response has been postulated to be due to inhomogenous,
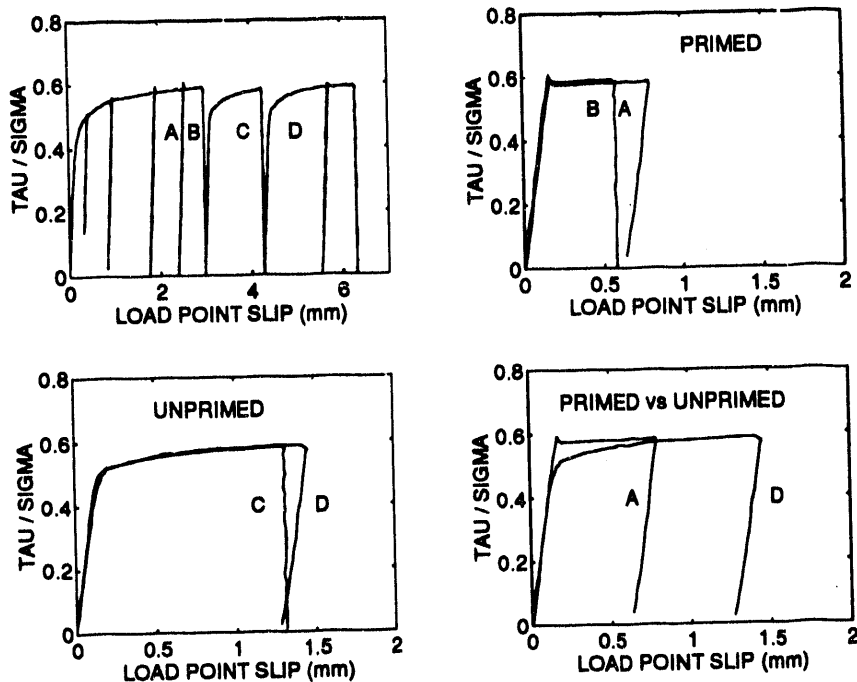
Figure 4: A stress-slip curve showing the different response for the same interface in the primed and unprimed states. Loops labelled A through D have been isolated to illustrate the concept of priming.

locked-in stress on the interface (Olsson, 1987b). In the Introduction, it was pointed out that peaks in the stress-slip curve due to velocity weakening can lead to instabilities in slip. The type of peak shown in Figure 4 is slip weakening and thus can also lead to instabilities.

The importance of primed versus unprimed joints lies in their different responses. By way of illustration, compare the sliding behavior of an *in situ* joint that has undergone some amount of shear during its history to that of the same joint cut out from its surroundings for either *in situ* or laboratory testing. The shear stiffness (defined as the slope of the stress-slip curve after the onset of slip) and strength of the tested joint will be less than its undisturbed counterpart, and the onset of slip will be more gradual and less prone to sudden slippage. Further, stability related response that may characterize the *in situ*, primed, joint will not be evident in data from the test specimem.

In geophysical applications, the concern centers around continual episodes of sliding separated by periods of stationary contact. Because the normal stress, in the experimental program, was approximately constant, the constitutive equations (2)–(10) seem to capture most of the important phenomena. Although zero velocity is a particular history of velocity, it is not clear whether these equations apply to loading of unprimed surfaces. It is important to explore this point because joints,
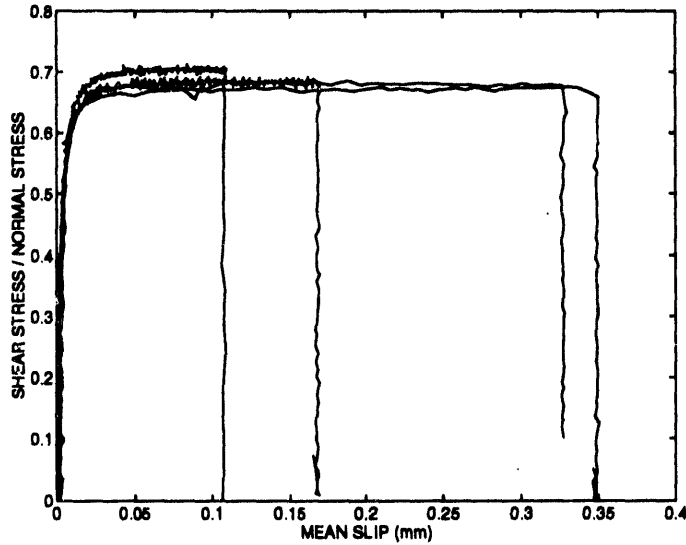
Figure 5: The stress-slip curves at different sliding velocities for unprimed surfaces. All experiments started at the same initial placement and at 5 MPa normal stress.

unlike faults, have not undergone large displacements.

3.1.1 Unprimed surfaces

To measure the effects of sliding velocity on the response of unprimed surfaces, the joint was slid at a constant velocity to a preselected total slip, then the shear stress and the normal stress were reduced to zero, and then the joint returned to zero slip. Next the normal stress was reapplied, and the joint reloaded in shear and subsequently unloaded as before. This was repeated at each desired velocity, always starting from the same relative position. Between each experiment, the sample was cleaned of gouge with a blast of compressed air. In this way the effect of sliding at four different velocities for an unprimed surface was measured. The velocities were varied by decades from 0.1 μm/s to 100 μm/s. The results are shown in Figure 5.

The curves from experiments at lower velocities have a "fuzzy" aspect caused by digital noise, and this is insignificant. Irrespective of velocity, each curve has the same shape. They all become nonlinear in the neighborhood of $\mu = 0.5$ and then roll over to the steady friction within 0.05mm of slip. The steady friction is function of the velocity—the higher the velocity, the lower the friction. These data are summarized below as "constant rate, unprimed" in Figure 7.

Because the joint remains in stationary contact while being loaded to slip at different velocities, the initial (vertical) parts of the curves also represent displacement hold tests with differing hold

8
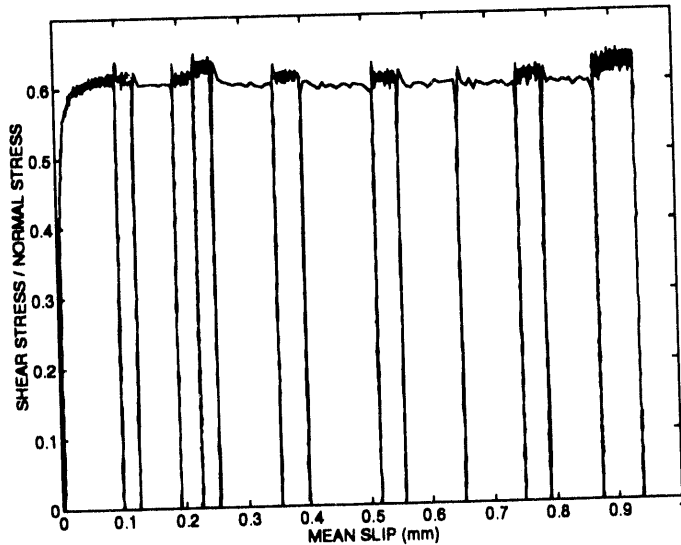
Figure 6: The effect of sliding velocities (indicated in μm/sec) on a primed surface. Note the differences between the way slip develops in these experiments with those of an unprimed surface shown in Figure 1.

times on unprimed joints. It has been observed that friction increases during nominally stationary contact of granite (Dieterich, 1972) and welded tuff (Teufel, 1981). Those tests were done in the primed condition and, therfore, it is interesting to examine the possibility of time-dependent strengthening for the unprimed surfaces as tested here. The hold times corresponding to load-point velocities of 0.1, 1, 10, and 100 μm/s were, respectively, 7.75, 31.3, 172, 1203 seconds. These hold times spanned the same range as those applied to a primed surface, as discussed in sections 3.2 and 4.2. The lack of any apparent effect of different hold times, especially the appearance of a peak, is to be contrasted with the results presented below for slide-hold-slide experiments on a primed joint.

3.1.2 Primed surfaces

Figure 6 illustrates the effects of different sliding velocities on a primed joint. At the beginning (when the surface is unprimed) the stress increases and rolls over smoothly. At 0.1 mm of slip, the shear stress was reduced to zero and again increased at the same rate (1 μm/s). This time, the stress rises to a peak and then rapidly descends to the steady value. Each successive cycle on the now primed surface shows a similar peak and distinct, lower, sliding stress that depends on the applied velocity. Each vertical segment represents unloading at the load-point velocity of 1 μm/s, and loading at the new load-point velocity. Note that each loading phase is a hold-time test for
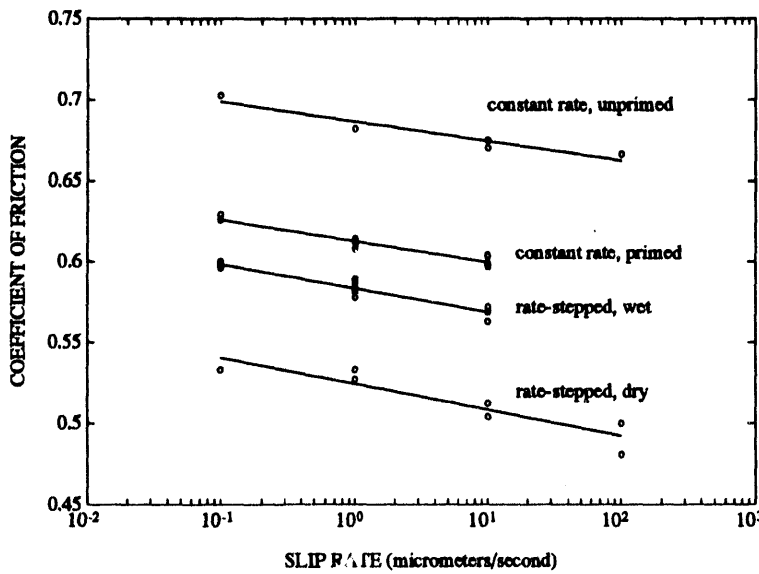
Figure 7: Rate sensitivities of the steady-state friction coefficient for various initial conditions.

each of the different velocities for a primed surface. The response now is typical for loading of primed surfaces—there exists a peak in the stress-slip curve, which decays rapidly with slip to a steady-state value. The steady portion is rate dependent and these data are included in Figure 7 as "constant rate, primed".

Data from previous rate-stepping (as sketched in Figure 1) experiments (Olsson, 1987a, 1988a) on dry surfaces, and new data from a surface submerged in room-temperature tap water are also plotted in Figure 7. The rate-stepping experiments are by their very nature carried out on primed surfaces. The greater friction for the wet surface compared to the dry surface was also found in an earlier study on a different tuff (Teufel, 1982). It appears that the steady-state friction of an unprimed surface is greater than that for a primed surface. An important aspect of Figure 7 is the parallelism of the various lines. These data give $a - b \approx 0.014$ for smooth, bare surfaces of Topopah Spring Member tuff; this is about 3 times that value observed for granites.

Another aspect of time-dependent joint slip is shown in Figure 8. Here the remote velocity V_0 is held at zero for different lengths of time after some sliding (Fig. 9). Between each test $V_0 = 5\mu m/s$. The strengthening during displacement holds was suggested (Dieterich, 1972) to be related to growth of asperity area during stationary contact. Ruina (1983), however, asserts that the strengthening is a result of small amounts of slip that take place while the load point is stationary, rather than the time during which the joint walls are in stationary contact. With regard to equation (3), for $V_0 = 0$, no evolution of state (strengthening) is predicted to occur. Dieterich (1981) used a different formulation for Ψ that does predict static strengthening. However, the data presented here suggest that in the absence of nonzero load-point shear stress (unprimed), no stress peaks

10
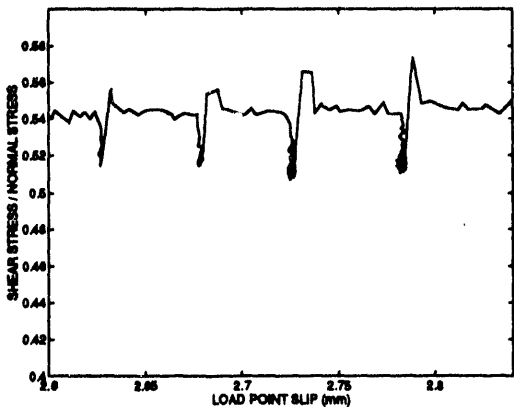
Figure 8: Variation of friction in a slide-hold-slide test. Note the stress-relaxation at each displacement hold, and the transient strengthening.

reflecting time-dependent strengthening develop. If Ruina's assertion is correct, then there must be some very small amount of slip occurring in the primed, stationary phases. Evidently, the amount of slip must be smaller than the slip resolution of the equipment used here (Fig. 8).

Both the static portions of the rate tests on an unprimed surface (Fig. 5) and on the primed surface (Fig. 6) are accompanied by an increasing shear stress. Thus, one might expect some microscopic slippage, which by Ruina's argument should lead to peaked curves resulting from strengthening. The lack of stress peak development in the unprimed surface condition, indicates that there is something more to it. The main difference is that the rate tests on the primed surface are preceded by a steady-state sliding phase that is not terminated by a momentary removal of the normal stress. Thus, it appears that when the normal stress is allowed to go to zero, the memory of that past slip history, which is reflected in $\Psi = 0$, is erased.

4 Creep

Creep is defined just as it is for solid materials: deformation (in this instance slip) at constant stress. Creep tests were done on the surface in both initial states, unprimed and primed.

4.1 Unprimed Surface

A number of short-term (minutes to hours) creep tests at various stress levels were done on the unprimed surface. The load-point displacement was increased until the corresponding shear stress

11
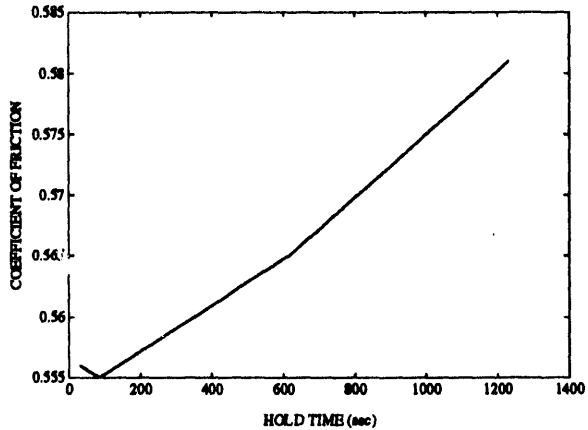
Figure 9: The effect of displacement holds of various lengths on the strength.

increased to a preselected level where the control mode was switched to load; i.e., the load point was maintained at constant load. No slip was recorded in any of these tests.

4.2 Primed Surface

Several creep tests conducted on a primed surface are shown in Figure 10. The small plot at the top of the figure shows the entire test record. Starting in the unprimed condition at $\sigma = 5$ MPa, the joint was slid at a constant velocity to about 0.14 mm, where the displacement was put in hold and the control mode switched to load. When the displacement was stopped, the stress relaxed, nearly instantaneously, to a little less than 0.6σ. Thus, this represents a constant stress test at about 95% of the sliding stress. No slip was observed in 2.5 hours, at which time the stress was raised to 0.617σ (about 99% of the slip stress). After something less than an hour, no creep was observed, so the stress was raised to 0.623σ, or greater than the stress required for sliding under dynamic conditions immediately preceding the creep experiments. Again, no creep was observed. Finally, the control mode was switched back to displacement and was increased at the former rate causing the stress to jump to 0.670σ before slip reinitiated and the stress rapidly resumed its former value. Evidently, microscopic slippage that occurs in association with the stress relaxation, leads to a strengthening, $a > 0$, that actually prevents classical creep. In fact, at $\mu = .623$, one whould expect, based on experience with creep of solids, accelerating creep.

12
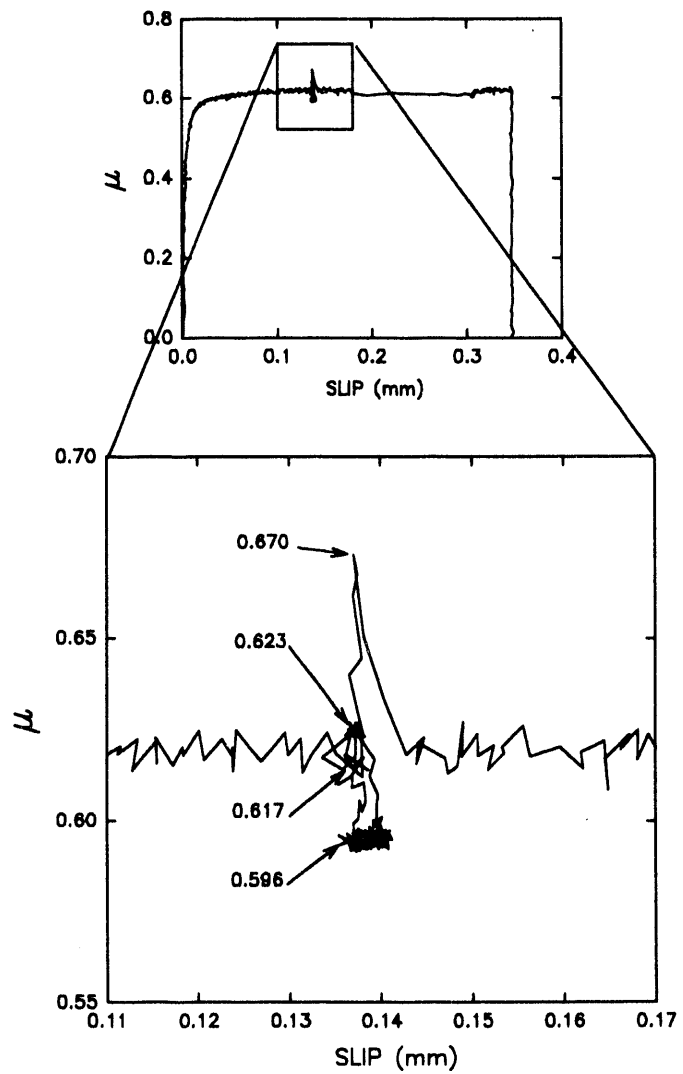
Figure 10: A creep test near the slip stress on a primed surface.

5 Conclusions

Rotary shear experiments at constant normal stress have been run on a smooth, artificial joint in Topopah Spring Member tuff. In general, this rock behaves much like other silicate rocks in its sensitivity to velocity changes and displacement history, but this program has highlighted some new and relatively unexplored behavior. Two initial states, unprimed and primed exhibit qualitatively and quantitatively different responses. The result that there are two limiting initial conditions, primed and unprimed, indicates that inferring rock mass response from *in situ* or laboratory properties could lead to errors without substantially improved understanding of the initial conditions of real joints. It is important to differentiate between the continued deformation of a joint that has been relieved of *in situ* stress from one that has not been.

In the steady-state friction regime, the slip behavior of this rock is well-described by the rate- and state-dependent constitutive law. Fractures in a steady-state exhibit velocity weakening at the low normal stresses used here, and $b - a \approx 0.014$. This type of constitutive reponse, in combination with the relatively low modulus of the rock mass compared with intact rock, and the well-known stress concentrations that occur in the vicinity of underground openings, suggests that dynamic instabilities may manifest themselves in the form of acoustic emissions or, possibly, higher amplitude events. These results indicate that acoustic monitoring of the repository may be useful from a safety standpoint.

Short-term creep tests in both the primed and unprimed states show no time-dependent slip. In the primed state, the shear stress to reinitiate slip after a nominal constant slip period, exceeds the immediately preceding steady-state value. Thus, some mechanism, either time-dependent strengthening of static friction, or friction increases due to microscopic slip as suggested by the rate- and state-dependent frcition law, is preventing slip at constant stress.

The effect of submerging the joint in water shows that the friction is higher for wet joints than dry ones, but that there is little difference in the trend or magnitude of the rate effect. Presumably, this results from the fact that the largest changes due to moisture occur in the first fractions of a percent of water content, and thus experiments run in the so-called laboratory air-dry (but still in ambient humidity) condition already have the necessary water content to behave similarly to saturated samples. Thus, conclusions based on air-dry samples will still pertain to joints *in situ*.

6 References

Blanpied, M. L., T. E. Tullis, J. D. Weeks, Frictional behavior of granite at low and high sliding velocities, *Geophys. Res. Let., 14*, 554–557, 1987. (NNA.900918.0009)

Blanpied, M. L., D. A. Lockner and J.D. Byerlee, Fault stability inferred from granite sliding experiments at hydrothermal condtions, *Geophy. Res. Let.*, *18*, 609–612, 1991. (NNA.930330.0073)

Brace, W. F., and J. D. Byerlee, Stick-slip as mechanism for earthquakes, *Science, 153*, 990–992, 1966. (NNA.930330.0074)

Christensen, R. J., S. R. Swanson, and W. S. Brown, Torsional shear measurements of the frictional properites of Westerly granite, in *Advances in Rock Mechanics, Proc. 3rd Cong. Intern. Soc. Rock Mech.*, 221–225, 1974. (NNA.900919.0172)

Dieterich, J. H., Time-dependent friction in rocks, *J. Geophys. Res, 77*, 3690–3697, 1972. (HQS.880517.1159)

Dieterich, J. H., Time-dependent friction and the mechanics of stick-slip, *Pageoph, 116*, 790–806, 1978. (HQS.880517.1161)

Dieterich, J. H., Modeling of rock friction: 1. Experimental results and constitutive equations, *J. Geophys. Res., 84*,2161–2168, 1979. (NNA.900918.0016)

Dieterich, J. H., Constitutive properites of faults with simulated gouge, in *Mechanical Behavior of Crustal Rocks: The Handin Volume, Geophys. Monogr. Ser., 24*, edited by N. L. Carter, M. Friedman, J. M. Logan, D. W. Strearns, 103–120, 1981. (NNA.900919.0173)

Dieterich, J. H., and G. Conrad, Effect of humidity on time- and velocity-dependent friction in rocks, *J. Geophysical Res., 89*, 4196–4202, 1981. (NNA.900918.0017)

Gu, J.-C., J. R. Rice, A. L. Ruina, and S. T. Tse, Slip motion and stability of a single degree of freedom elastic system with rate and state dependent friction, J. Mech. Phys. Solids, 32 , 167–196, 1984. (NNA.900918.0018)

Holcomb, D. J., and L. W. Teufel, Acoustic emissions during deformation of intact and jointed welded tuff, *Sandia National Laboratories Tech. Rep., SAND82-1003*, Albuquerque, NM, 1982. (SRX.820817.0119)

Kutter, H. K., Rotary shear testing of rock joints, in *Proc. 3rd Cong. of the Intern. Soc. for Rock Mech.*, National Academy of Sciences, Washington, D.C., 254–262, 1974. (NNA.900919.0174)

Marone, C., C. B. Raleigh, and C. H. Scholz, Frictional behavior and constitutive modeling of simulated fault gouge, *J. Geophys. Res., 95*, 7000–7025, 1990. (NNA.930330.0075)

Olsson, W. A., A dislocation model of the stress history dependence of frictional slip, *J. Geophys. Res., 89*, 9271–9280, 1984. (NNA.900403.0279)

Olsson, W. A., The effects of changes in normal stress on rock friction, in *Constitutive Laws for Engineering Materials: Theory and Applications*, ed. C. S. Desai, E. Krempl, P. D. Kiousis, T. Kundu, p. 1059–1066, Elsevier, New York, 1987a. (NNA.910207.0028)

Olsson, W. A., Rock Joint Compliance Studies, *Sandia National Laboratories Tech. Rep., SAND86-0177*, Albuquerque, NM, 1987b. (NNA.891019.0291)

Olsson, W. A., Compliance and Strength of Artificial Joints in Topopah Spring Tuff, *Sandia National Laboratories Tech. Rep., SAND88-0660*, Albuquerque, NM, 1988. (NNA.881202.0205)

Olsson, W. A., The effects of normal stress history on rock friction, in *Key Questions in Rock Mechanics: Proceedings of the 29th U.S. Symp. Rock Mechanics*, eds. P. A. Cundall, R. L. Sterling, and A. M. Starfield, 111–117, Balkema, Brookfield, 1988. (NNA.900403.0382)

Olsson, W. A., The effects of shear and normal stress paths on rock friction, in *Rock Joints: Proceedings of the International Symposium on Rock Joints*, eds. N. Barton and O. Stephansson, 475–479, Balkema, Brookfield, 1990. (NNA.900426.0053)

Olsson, W. A., The effect of slip on the flow of fluid through a fracture, *Geophys. Res. Let., 19*, 541–543, 1992. (NNA.930330.0076)

Olsson, W. A., and S. R. Brown, Hydromechanical response of a fracture undergoing compression and shear, accepted for publication in *Proc. 34th U. S. Symposium on Rock Mechanics*, 1993. (NNA.940301.0034)

Price, R. H., J. R. Connolly, and K. Keil, Petrologic and mechanical properties of outcrop samples of the welded, devitrified Topopah Spring Member of the Paintbrush tuff, *SAND86-1131*, Sandia National Laboratories, Albuquerque, NM, 1987. (HQS.880517.1704)

Rice, J. R., Constitutive relations for fault slip and earthquake instabilities, *PAGEOPH, 121*, 443–475, 1983. (NNA.930330.0077)

Rice, J. R., and J.-C. Gu, Earthquake aftereffects and triggered seismic phenomena, *PAGEOPH, 121*, 187–219, 1983. (NNA.930330.0078)

Rice, J. R. and A. L. Ruina, Stability of steady frictional slipping, J. Appl. Mech., 50, 343–349, 1983. (NNA.930414.0032)

Ruina, A., Friction laws and instabilities: a quasistatic analysis of some dry frictional behavior, Report No. 21 (Ph. D. Thesis), Division of Engineering, Brown University, Providence, R. I., 1980. (NNA.940301.0035)

Ruina, A., Slip instability and state variable friction laws, J. Geophys. Res., 88, 10,359–10,370, 1983. (NNA.930330.0079)

Teufel, L. W., Frictional properties of jointed welded tuff, *Sandia National Laboratories Tech. Rep., SAND81-0212*, Albuquerque, NM, 1982. (HQS.880517.2356)

Tullis, T. E., and J. D. Weeks, Constitutive behavior and stability of frictional sliding of granite, *PAGEOPH, 124*, 383–414, 1986. (NNA.930330.0080)

Weeks, J. D., and T. E. Tullis, Frictional sliding of dolomite: a variation in constitutive behavior, *J. Geophys. Res., 90*, 7821–7826, 1985. (NNA.930330.0081)

Wong, I. G., Recent developments in rockburst and mine seismicity research, in *Rock Mechanics*, Proc. 33rd U. S. Rock Mech. Symp., eds. J. R. Tillerson and W. R. Wawersik, 1103–1112, Balkema, Rotterdam, 1992. (NNA.930414.0033)

Xu, S. and M. H. de Frietas, Use of a rotary shear box for testing the shear strength of rock joints, *Geotechnique, 38*, 301–309, 1988. (NNA.900918.0012)

Yoshioka, N., and C. H. Scholz, Elastic properties of contacting surfaces under normal and shear loads 2. Comparison of theory with experiment, *J. Geophys. Res., 94*, 17691–17700, 1989. (NNA.900403.0393)

17

APPENDIX

Information from the Reference Information Base Used in this Report

This report contains no information from the Reference Information Base.

Candidate Information
for the
Reference Information Base

This report contains no candidate information for the Reference Information Base.

Candidate Information
for the
Geographic Nodal Information Study
and Evaluation System

This report contains no candidate information for the Geographic Nodal Information Study and Evaluation System.

YUCCA MOUNTAIN SITE CHARACTERIZATION PROJECT

DISTRIBUTION LIST

1 D.A. Dreyfus (RW-1)
Director
OCRWM
US Department of Energy
1000 Independence Avenue SW
Washington, DC 20585

1 L.H. Barrett (RW-2)
Acting Deputy Director
OCRWM
US Department of Energy
1000 Independence Avenue SW
Washington, DC 20585

1 J.D. Saltzman (RW-4)
Office of Strategic Planning and
 International Programs
OCRWM
US Department of Energy
1000 Independence Avenue SW
Washington, DC 20585

1 J.D. Saltzman (RW-5)
Office of External Relations
OCRWM
US Department of Energy
1000 Independence Avenue SW
Washington, DC 20585

1 Samuel Rousso (RW-10)
Office of Program and Resource Mgt.
OCRWM
US Department of Energy
1000 Independence Avenue SW
Washington, DC 20585

1 J. C. Bresee (RW-10)
OCRWM
US Department of Energy
1000 Independence Avenue SW
Washington, DC 20585

1 R.M. Nelson (RW-20)
Office of Geologic Disposal
OCRWM
US Department of Energy
1000 Independence Avenue, SW
Washington, DC 20585

1 S. J. Brocoum (RW-22)
Analysis and Verification Division
OCRWM
US Department of Energy
1000 Independence Avenue SW
Washington, DC 2585

1 D. Shelor (RW-30)
Office of Systems and Compliance
OCRWM
US Department of Energy
1000 Independence Avenue, SW
Washington, DC 20585

1 J. Roberts (RW-33)
Director, Regulatory Compliance
 Division
OCRWM
US Department of Energy
1000 Independence Avenue, SW
Washington, DC 20585

1 G. J. Parker (RW-332)
Reg. Policy/Requirements Branch
OCRWM
US Department of Energy
1000 Independence Avenue, SW
Washington, DC 20585

1 R. A. Milner (RW-40)
Office of Storage and
 Transportation
OCRWM
US Department of Energy
1000 Independence Avenue, SW
Washington, DC 20585

1	S. Rousso (RW-50) Office of Contract Business Management OCRWM US Department of Energy 1000 Independence Avenue, SW Washington, DC 20585	1	D. R. Elle, Director Environmental Protection and Division DOE Nevada Field Office US Department of Energy P.O. Box 98518 Las Vegas, NV 89193-8518
1	T. Wood (RW-52) Director, M&O Management Division OCRWM US Department of Energy 1000 Independence Avenue, SW Washington, DC 20585	1	Repository Licensing & Quality Assurance Project Directorate Division of Waste Management US NRC Washington, DC 20555
4	Victoria F. Reich, Librarian Nuclear Waste Technical Review Board 1100 Wilson Blvd, Suite 910 Arlington, VA 22209	1	Senior Project Manager for Yucca Mountain Repository Project Branch Division of Waste Management US NRC Washington, DC 20555
5	R.M. Nelson Jr, Acting Project Manager Yucca Mountain Site Characterization Project Office US Department of Energy P.O. Box 98608--MS 523 Las Vegas, NV 89193-8608	1	NRC Document Control Desk Division of Waste Management US NRC Washington, DC 20555
1	C. L. West, Director Office of External Affairs DOE Nevada Field Office US Department of Energy P.O. Box 98518 Las Vegas, NV 89193-8518	1	Philip S. Justus NRC Site Representive 301 E Stewart Avenue, Room 203 Las Vegas, NV 89101
8	Technical Information Officer DOE Nevada Field Office US Department of Energy P.O. Box 98518 Las Vegas, NV 89193-8518	1	E. P. Binnall Field Systems Group Leader Building 50B/4235 Lawrence Berkeley Laboratory Berkeley, CA 94720

1	P. K. Fitzsimmons, Technical Advisor
	Office of Assistant Manager for
	  Environmental Safety and
	  Health
	DOE Nevada Field Office
	US Department of Energy
	P.O. Box 98518
	Las Vegas, NV 89193-8518
		1	Center for Nuclear Waste
			  Regulatory Analyses
			6220 Culebra Road
			Drawer 28510
			San Antonio, TX 78284

		3	W. L. Clarke Technical Project Officer - YMP Attn: YMP/LRC Lawrence Livermore National Laboratory P.O. Box 5514 Livermore, CA 94551

1	J. A. Blink
	Deputy Project Leader
	Lawrence Livermore National
	  Laboratory
	101 Convention Center Drive
	Suite 820, MS 527
	Las Vegas, NV 89109
			1	V. R. Schneider
				Asst. Chief Hydrologist--MS 414
				Office of Program Coordination
				  and Technical Support
				US Geological Survey
				12201 Sunrise Valley Drive
				Reston, VA 22092

4	J. A. Canepa Technical Project Officer - YMP N-5, Mail Stop J521 Los Alamos National Laboratory P.O. Box 1663 Los Alamos, NM 87545		1	J. S. Stuckless Geologic Division Coordinator MS 913 Yucca Mountain Project US Geological Survey P.O. Box 25046 Denver, CO 80225
1	H. N. Kalia Exploratory Shaft Test Manager Los Alamos National Laboratory Mail Stop 527 101 Convention Center Dr., #820 Las Vegas, NV 89101		1	D. H. Appel, Chief Hydrologic Investigations Program MS 421 US Geological Survey P.O. Box 25046 Denver, CO 80225
1	N. Z. Elkins Deputy Technical Project Officer Los Alamos National Laboratory Mail Stop 527 101 Convention Center Dr., #820 Las Vegas, NV 89101		1	E. J. Helley Branch of Western Regional Geology MS 427 US Geological Survey 345 Middlefield Road Menlo Park, CA 94025
5	L. E. Shephard Technical Project Officer - YMP Sandia National Laboratories Organization 6302 P.O. Box 5800 Albuquerque, NM 87185		1	R. W. Craig, Chief Nevada Operations Office US Geological Survey 101 Convention Center Drive Suite 860, MS 509 Las Vegas, NV 89109
1	J. F. Devine Asst Director of Engineering Geology US Geological Survey 106 National Center 12201 Sunrise Valley Drive Reston, VA 22092		1	D. Zesiger US Geological Survey 101 Conventional Center Drive Suite 860, MS 509 Las Vegas, NV 89109
1	L. R. Hayes Technical Project Officer Yucca Mountain Project Branch MS 425 US Geological Survey P.O. Box 25046 Denver, CO 80225		1	G. L. Ducret, Associate Chief Yucca Mountain Project Division US Geological Survey P.O. Box 25046 421 Federal Center Denver, CO 80225

1	A. L. Flint US Geological Survey MS 721 P.O. Box 327 Mercury, NV 89023	2	L. D. Foust Nevada Site Manager TRW Environmental Safety Systems 101 Convention Center Drive Suite 540, MS 423 Las Vegas, NV 89109
1	D. A. Beck Water Resources Division, USGS 6770 S Paradise Road Las Vegas, NV 89119	1	C. E. Ezra YMP Support Office Manager EG&G Energy Measurements Inc MS V-02 P.O. Box 1912 Las Vegas, NV 89125
1	P. A. Glancy US Geological Survey Federal Building, Room 224 Carson City, NV 89701	1	E. L. Snow, Program Manager Roy F. Weston Inc 955 L'Enfant Plaza SW Washington, DC 20024
1	Sherman S.C. Wu US Geological Survey 2255 N. Gemini Drive Flagstaff, AZ 86001	1	Technical Information Center Roy F. Weston Inc 955 L'Enfant Plaza SW Washington, DC 20024
1	J. H. Sass - USGS Branch of Tectonophysics 2255 N Gemini Drive Flagstaff, AZ 86001	1	D. Hedges, Vice President, QA Roy F. Weston Inc 4425 Spring Mountain Road Suite 300 Las Vegas, NV 89102
1	DeWayne Campbell Technical Project Officer - YMP US Bureau of Reclamation Code D-3790 P.O. Box 25007 Denver, CO 80225	1	D. L. Fraser, General Manager Reynolds Electrical & Engineering Co, Inc MS 555 P.O. Box 98521 Las Vegas, NV 89193-8521
1	J. M. LaMonaca Records Specialist US Geological Survey 421 Federal Center P.O. Box 25046 Denver, CO 80225	1	B. W. Colston, President and General Manager Las Vegas Branch Raytheon Services Nevada MS 416 P.O. Box 95487 Las Vegas, NV 89193-5487
1	W. R. Keefer - USGS 913 Federal Center P.O. Box 25046 Denver, CO 80225		
1	M. D. Voegele Technical Project Officer - YMP SAIC 101 Convention Center Drive Suite 407 Las Vegas, NV 89109	1	R. L. Bullock Technical Project Officer - YMP Raytheon Services Nevada Suite P-250, MS 403 101 Convention Center Drive Las Vegas, NV 89109

1   Paul Eslinger, Manager
PASS Program
Pacific Northwest Laboratories
P.O. Box 999
Richland, WA 99352

1   A. T. Tamura
Science and Technology Division
OSTI
US Department of Energy
P.O. Box 62
Oak Ridge, TN 37831

1   Carlos G. Bell Jr
Professor of Civil Engineering
Civil and Mechanical Engineering Dept.
University of Nevada, Las Vegas
4505 S Maryland Parkway
Las Vegas, NV 89154

1   P. J. Weeden, Acting Director
Nuclear Radiation Assessment Div.
US EPA
Environmental Monitoring
  Systems Lab
P.O. Box 93478
Las Vegas, NV 89193-3478

1   ONWI Library
Battelle Columbus Laboratory
Office of Nuclear Waste Isolation
505 King Avenue
Columbus, OH 43201

1   T. Hay, Executive Assistant
Office of the Governor
State of Nevada
Capitol Complex
Carson City, NV 89710

3   R. R. Loux
Executive Director
Agency for Nuclear Projects
State of Nevada
Evergreen Center, Suite 252
1802 N. Carson Street
Carson City, NV 89710

1   C.H. Johnson
Technical Program Manager
Agency for Nuclear Projects
State of Nevada
Evergreen Center, Suite 252
1802 N. Carson Street
Carson City, NV 89710

1   John Fordham
Water Resources Center
Desert Research Institute
P.O. Box 60220
Reno, NV 89506

1   David Rhode
Desert Research Institute
P.O. Box 60220
Reno, NV 89506

1   Eric Anderson
Mountain West Research-
  Southwest Inc
2901 N Central Avenue #1000
Phoenix, AZ 85012-2730

1   The Honorable Cyril Schank
Chairman
Churchill County Board of
  Commissioners
190 W First Street
Fallon, NV 89406

1   Dennis Bechtel, Coordinator
Nuclear Waste Division
Clark County Department of
  Comprehensive Planning
301 E Clark Avenue, Suite 570
Las Vegas, NV 89101

1   Juanita D. Hoffman
Nuclear Waste Repository
  Oversight Program
Esmeralda County
P.O. Box 490
Goldfield, NV 89013

1   Eureka County Board of Commissioners
Yucca Mountain Information
  Office
P.O. Box 714
Eureka, NV 89316

1	Brad Mettam Inyo County Yucca Mountain Repository Assessment Office Drawer L Independence, CA 93526	1	Economic Development Dept. City of Las Vegas 400 E. Stewart Avenue Las Vegas, NV 89101

1	Lander County Board of
	  Commissioners
	315 South Humbolt
	Battle Mountain, NV 89820
		1	Commmunity Planning and
			  Development
			City of North Las Vegas
			P.O. Box 4086
			North Las Vegas, NV 89030

1	Vernon E. Poe Office of Nuclear Projects Mineral County P.O. Box 1026 Hawthorne, NV 89415	1	Community Development and Planning City of Boulder City P.O. Box 61350 Boulder City, NV 89006

1	Les W. Bradshaw
	Program Manager
	Nye County Nuclear Waste
	  Repository Program
	P.O. Box 153
	Tonopah, NV 89049
		1	Commission of the European
			  Communities
			200 Rue de la Loi
			B-1049 Brussells
			BELGIUM

1	Florindo Mariani
	White Pine County Nuclear
	  Waste Project Office
	457 Fifth Street
	Ely, NV 89301
		2	M. J. Dorsey, Librarian
			YMP Research and Study Center
			Reynolds Electrical &
			  Engineering Co Inc
			MS 407
			P.O. Box 98521
			Las Vegas, NV 89193-8521

1	Judy Foremaster
	  City of Caliente Nuclear Waste
	  Project Office
	P.O. Box 158
	Caliente, NV 89008
		1	Amy Anderson
			Argonne National Laboratory
			Building 362
			9700 S Cass Avenue
			Argonne, IL 60439

1	Phillip A. Niedzielski-Eichner Nye County Nuclear Waste Repository Project Office P.O. Box 221274 Chantilly, VA 22022-1274	1	Steve Bradhurst P.O. Box 1510 Reno, NV 89505
1	Jason Pitts Lincoln County Nuclear Waste Project Office Lincoln County Courthouse Pioche, NV 89043	1	Michael L. Baughman 35 Clark Road Fiskdale, MA 01518
		1	Glenn Van Roekel Director of Community Development City of Caliente P.O. Box 158 Caliente, NV 89008

1	Ray Williams, Jr
	P.O. Box 10
	Austin, NV 89310

1   Nye County District Attorney
P.O. Box 593
Tonopah, NV 89049

1   William Offutt
Nye County Manager
Tonopah, NV 89049

1   Charles Thistlethwaite, AICP
Associate Planner
Inyo County Planning Department
Drawer L
Independence, CA 93526

1   R. F. Pritchett
Technical Project Officer - YMP
Reynolds Electrical &
   Engineering Company Inc
MS 408
P.O. Box 98521
Las Vegas, NV 89193-8521

1   Dr. Moses Karakouzian
1751 E Reno #125
Las Vegas, NV 89119

1   Michael L. Blanpied
USGS
MS 977
345 Middlefield Road
Menlo Park, CA 94024

1   James H. Dieterich
USGS
MS 977
345 Middlefield Road
Menlo Park, CA 94024

1   C. Scholtz
Lamont-Doherty Geo.
   Observatory
Palisades, NY 10964

1   Professsor Terry Tullis
Dept of Geological Sciences
Brown University
Providence, RI 02912

1   Dr. John Weeks
Dept of Geological Sciences
Brown University
Providence, RI 02912

	MS	
1	1325	L.S. Costin, 6313
2	1330	G.M. Gerstner-Miller, 6352
		100/1232714/SAND92-2333/QA
2	1330	G.M. Gerstner-Miller, 6352
		DRMS Files (Data Set 51/L02-06/04/84)
20	1330	WMT Library, 6352
1	1324	P.B. Davies, 6115
1	0827	P.J. Hommert, 1502
1	1375	D.A. Dahlgren, 4400
5	0899	Technical Library, 7141
1	0619	Technical Publications, 7151
10	1119	Document Processing for DOE/OSTI, 7613-2
1	9018	Central Technical Files, 8523-2
1	0751	W.R. Wawersik, 6117
1	0751	S.R. Brown, 6117
1	0751	J.T. Fredrick, 6117
20	0751	W.A. Olsson, 6117
10	1325	R.H. Price, 6313

SAND92-2333

The number in the lower right-hand corner
is an accession number used for Office of
Civilian Radioactive Waste Management
purposes only. It should not be used
when ordering this publication.

NNA.940209.0001

END

DATE FILMED

5/12/94